



The Effects of the Specific Material Selection on the Structural Behaviour of the Piston-Liner Coupling of a High Performance Engine

Saverio Giulio Barbieri, Valerio Mangeruga, and Matteo Giacopini University of Modena and Reggio Emilia

Citation: Barbieri, S.G., Mangeruga, V., and Giacopini, M., "The Effects of the Specific Material Selection on the Structural Behaviour of the Piston-Liner Coupling of a High Performance Engine," SAE Technical Paper 2021-01-1235, 2021, doi:10.4271/2021-01-1235.

ABSTRACT

The materials commonly employed in the automotive industry are various and depend on the specific application field. For what concern the internal combustion engines the choice is guided by the thermomechanical performance required, technological constraints and production costs. Actually, for high-performance engines, steel and aluminium are the most common materials selected for the piston and the cylinder liner manufacturing. This study analyses the effect of possible material choice on the interaction between piston and cylinder liner, via Finite Element analyses. A motorcycle engine is investigated considering two possible pistons: one (standard) made of aluminium and one made of steel. Similarly, two possible cylinder liners are considered, the original one made of aluminium and a different version made of steel obtained by simply thinning the aluminium component in order to obtain two structurally equivalent components. In particular, four possible

combinations of coupling between piston and cylinder liner are identified, derived from the two variants of applied materials. The components theoretically necessary for the Finite Element model are the engine head, the engine block, the bolts, the gasket, the upper part of the crank mechanism and the cylinder liner. Nevertheless, a simplified methodology is employed to reduce the computational effort. This analysis makes it possible to evaluate gap and interference with respect to the material choice. A first proposal of the barrel shape and ovality of the steel piston is obtained starting from the original aluminium piston and the thermal field involved in the analysis. Besides, the presented methodology consists of a useful tool to estimate the stress field and the fatigue safety factor of the components involved. The results obtained with this methodology can guide the definition of the correct piston profile, temperature field and stress distribution estimation, as a function of the specific materials employed for piston-liner coupling.

Introduction

The piston is a crucial element in the transmission of power [1]. In the combustion chamber of an engine, the chemical energy contained in the fuel is rapidly converted into heat and pressure during the combustion phase. The piston, which is the moving part of the combustion chamber, has to convert this energy into mechanical work. The most important tasks that the piston must fulfil are: to transmit force from the working gas (power stroke) and to the working gas (compression stroke), to be the variable lower bounding for the combustion chamber and to seal it, to guide the connecting rod, to dissipate heat, to support (in four-stroke engines) or to control (in two-stroke engines) the charge exchange, to support the mixture formation and to house the ring pack. Therefore, the most common requirements are high structural strength, adaptability to operating conditions, low friction, low wear, low oil consumption and low pollutant emissions. It is obvious that a proper material choice for this component is fundamental to meet these tasks [2, 3, 4].

Nevertheless, almost the whole road vehicles circulating nowadays adopt pistons made of aluminium. The only exceptions are present in fields far from series applications: in slow

Diesel engines, cast iron is used, while, in competitions, magnesium alloys are employed, which have less density, but also less resistance and a high friction coefficient combined to the other engine components.

On one hand, aluminium exhibits low density, low friction coefficient with the cylinder liner and a good heat dispersion thanks to its high value of thermal conductivity. On the other hand, the high value of its thermal expansion coefficient might cause blow-by during the cold start phase, thus resulting in not being able to fulfil the recent pressing emission norms. Moreover, the mechanical properties of aluminium collapse above 300°C and its high value of thermal conductivity negatively affects the adiabatic efficiency of the combustion chamber, even if a high value of thermal conductivity might help the temperature of the piston to be controlled.

Steel could be a much more suitable material for any kind of piston regardless of its specific usage. In particular, steel presents a low thermal expansion coefficient, thus resulting in a cold shape of the piston more similar to the one reached during the operating conditions, if compared to an aluminium piston [5]. In addition, steel exhibits a low thermal conductivity, which can positively affect the adiabatic efficiency of

the combustion chamber. Even if this last property could lead to high values of temperature of the piston, it should not be a critical issue, in fact, steel exhibits high structural strength also at high temperatures, up to 500–600°C [6]. Finally, Young modulus of steel is about three times Young modulus of aluminium. Therefore, comparable stiffness could be obtained by lowering thicknesses of the different parts of the piston thus allowing the steel piston to exhibit a comparable weight of the aluminium one.

All this considered, steel appears to be a much more suitable material for pistons than aluminium, nevertheless, aluminium is the most used material and steel is quite absent in the automotive landscape. If the production technologies are considered, the answer to this contradiction can be easily found, in fact, the most common manufacturing techniques are casting and forging. If a steel piston has to be designed starting from the geometry of a typical aluminium one, all the geometrical dimensions should be drastically reduced to achieve a steel piston with both mass and stiffness comparable to those of the original aluminium piston. Unfortunately, these very thin features cannot be produced using the most common production technologies, and the most recent ones should be adopted, such as Additive Manufacturing techniques [7].

The cylinder liner is another important element in the transmission of power [8]. Its main goals are to support the lateral force of the piston, to provide a good wear surface for the piston rings and to maintain cylindricity to aid piston rings sealing. If the inner surface of the liner deviates from the theoretical cylindrical shape because of the static loading of the bolt tightening or because of thermal stresses, the engine will experience higher oil consumption, higher blow-by, and higher friction losses [9]. Talking about the cooling system, the general approaches to the cylinder liner are integral liner, dry liner, and wet liner. In the present paper, the latter solution is taken into account, in fact, most of the heavy-duty diesel engines and (high performance) gasoline engines use wet liners. In such engines, the cylinder liners are pressed or slip fitted into the surrounding structure such that they are in direct contact with the coolant and sealed at the top and bottom. In order to provide sufficient structural stiffness, the block casting includes walls separating the cooling jackets for each cylinder. Wet liner engines holds the advantages of having the cylinders easily replaced when the engine is rebuilt, and direct contact of the cylinders with coolant for optimum temperature control. However, the cylinder spacing and thus the overall length of the engine must be increased, and also the possibility of coolant leakage raises. Aluminium is the most employed material for cylinder blocks of high-performance engines, in particular, this material shows a combination of good thermal conductivity, low-density, good machinability, and good mechanical properties [10]. When the wet liner solution is adopted, the designer is not forced to use aluminium also for the cylinder liner, and steel could be also employed especially when the main task of the liner is focused on mechanical strength.

When the design of a combustion engine with wet liners is considered, the engineers must decide which material, aluminium or steel, should be employed for the piston and for the cylinder liner, which, together, represent the core of

TABLE 1 Engine data.

Engine configuration	L-twin
Displacement	955 cm ³
Bore	100 mm
Stroke	60.8 mm
Maximum power	157 HP @ 11000 rpm
Maximum torque	107 Nm @ 9000 rpm
Maximum chamber pressure	91 bar

the transmission of power in an internal combustion engine. In addition, it is vital to understand how these components interact with each other when different materials are adopted. In detail, four different configurations are possible:

1. aluminium piston and aluminium liner;
2. aluminium piston and steel liner;
3. steel piston and aluminium liner;
4. steel piston and steel liner.

In the literature, the piston liner coupling has been widely investigated. Some researchers focused on the effect of different materials on the piston without modifying the geometry of the component [11]. Other studies dealt with the analysis and the design of the piston profile to reduce the piston secondary motion and friction [12,13] without debating the consequences of a different material on the design of the piston skirt profile.

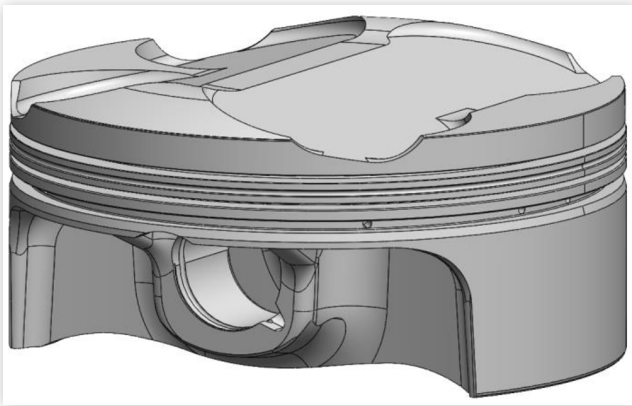
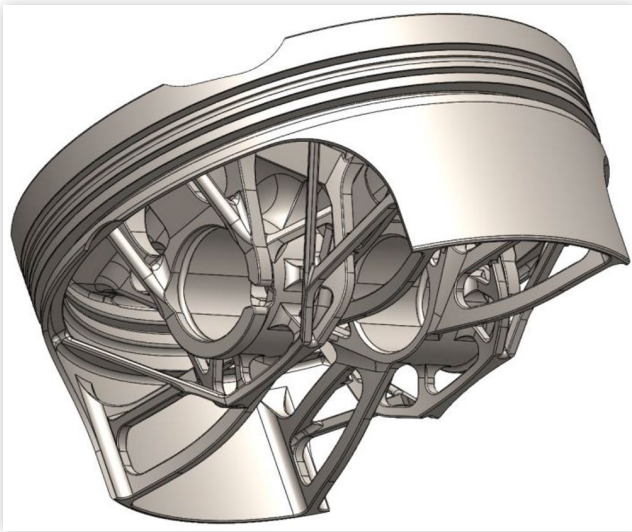
The present paper analyses the effect of the specific material selection on the structural behaviour of the piston-liner coupling of a high-performance gasoline engine. In particular, a methodology to obtain the first design proposal of these components is exposed.

Table 1 collects the main data of the engine under investigation, which is an L-twin high-performance four-stroke internal combustion engine for motorbike application. This engine is currently equipped with aluminium pistons and aluminium cylinder liners.

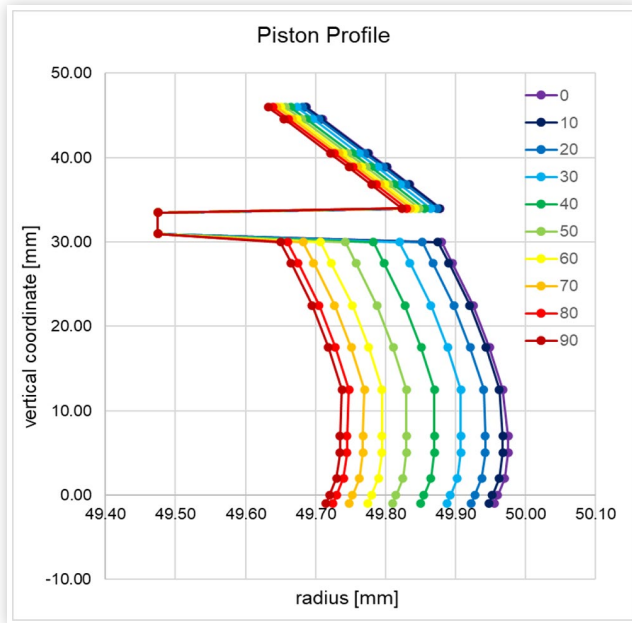
The paper is organized as follows. First, the design process of the steel piston is presented. In particular, the methodology adopted to obtain a first proposal of the piston profile is described in detail. In the following section, the definition of the geometries of the new steel liner is considered based on structural fatigue strength considerations. In the end, the Finite Element calculations related to the four possible cases of material selection are described and their results are presented. For each case, the most important outcomes are the values of the contact pressure, the extent and location of the contact area of the piston skirt and the detection (estimation) of gap or overclosure between the piston and the liner during the cold start phase.

Steel Piston Design Process

Figure 1 shows the original aluminium piston of the engine considered. It is produced by forging and it exhibits all the classical geometrical features typical of high-performance

FIGURE 1 The original aluminium piston.**FIGURE 2** The new steel piston.

gasoline engines, such as very marked valve pockets, a tight piston ring land area and a skirt with a quite narrow extent. As previously mentioned, to properly design and produce a new steel piston, Additive Manufacturing techniques could be adopted. When these recent technologies are taken into account, wide geometrical freedom is given to the engineer so that it is more advisable to conceive new geometries and to disengage from the traditional shape of the aluminium pistons. Therefore, it is necessary to employ a design methodology based on mathematical and engineering assumptions. Model-based approaches are widely discussed in the literature and reveal themselves to be well suitable for the automotive industry [14]. The methodology accomplished to design the new steel piston is widely described in [15, 16], at which the interest reader is referred. The new steel piston, see Figure 2, is structurally equivalent to the original aluminium one in term of stiffness of the piston top and skirt and the design process has been driven by Topology Optimization techniques. However, the contact interaction between the piston and the cylinder liner has not been investigated in detail. The present paper aims at closing this gap and also at deepening this theme.

FIGURE 3 The profile of the aluminium piston.

The piston outer geometry cannot properly be defined by the simple nominal bore. Figure 3 shows typical curves necessary to define the profile of the original aluminium piston addressed in this contribution. Each curve depicts the vertical coordinate as a function of the radius and each curve refers to a different angular position along the circumferential direction (only an amplitude of 90° has been considered since the profile of the piston is supposed to exhibit two symmetry planes). The 0° position refers to the midpoint of the skirt whilst the 90° position indicates the intersection with the axis of the gudgeon pin, where the skirt is almost totally absent. Referring to any curve of Figure 3, the vertical coordinates between 46 mm and 34 mm describe a truncated cone shape of the upper piston lands, while the vertical coordinates between 33 mm and 31 mm describe the land supporting the oil control ring, which shows a conspicuous reduction of the radius. Moving to the lower part of the profile related to the skirt, the so-called barrel shape of the piston is evident. If different curves are considered, it is easy to notice an overall reduction of the radius moving from the skirt midpoint to the axis of the pin; in particular, an elliptical (oval) shape is present moving around the piston. This particular elliptical geometry has the purpose to guarantee a geometry as circular as possible during the operating condition to allow a suitable piston-liner interaction. In fact, a different thermal deformation of the piston exists between the pin axis direction and the thrust-antithrust direction.

All these details of the piston profile have the task to confine to the skirt area the contact area between the piston and the liner. In detail, the truncated cone and the barrel shape should counteract the inhomogeneous thermal deformation of the piston moving along the vertical axis as a consequence of the strong thermal gradient present along the same direction.

All this considered, a fundamental consideration is that the profile of the original aluminium piston is suitable for the engine considered. Therefore, the first step of this research is to define the profile of the new steel piston so that the two pistons exhibit close profiles during the operating conditions.

Thermal Analysis of Aluminium Piston

First of all, the temperature field of the original aluminium piston has been deduced using a Finite Elements simulation. The methodology employed by the authors has been previously validated in [17] versus experimental evidence for a similar engine.

Table 2 collects both the thermal and mechanical properties of the materials used to feed numerical models, while Table 3 collects the thermal boundary conditions estimated and then applied to the single components for a revving speed equal 11000 rpm (corresponding to maximum power condition).

The commercial software Altair Hypermesh has been employed for the preprocessing phase, while MSC Marc has been adopted for the calculations. About 620 thousand elements have been employed: 73 thousand pentahedral elements (bilinear, 6 nodes, 6 Gaussian integration points), 47 thousand hexahedral elements (bilinear, 8 nodes, 8 Gaussian integration points) and 500 thousand tetrahedral elements (first order, 4 nodes, one Gaussian integration points), the average element size being 1 mm.

Figure 4 shows the result of the thermal calculation. Only one half of the upper part of the crank mechanism has been modelled taking advantage of the existing symmetry plane of the problem. Figure 5 focuses on the piston: a maximum temperature of about 300°C is registered on the crown. The skirt exhibits a minimum temperature of 110°C and this huge thermal gradient strongly affects the deformed shape of the piston.

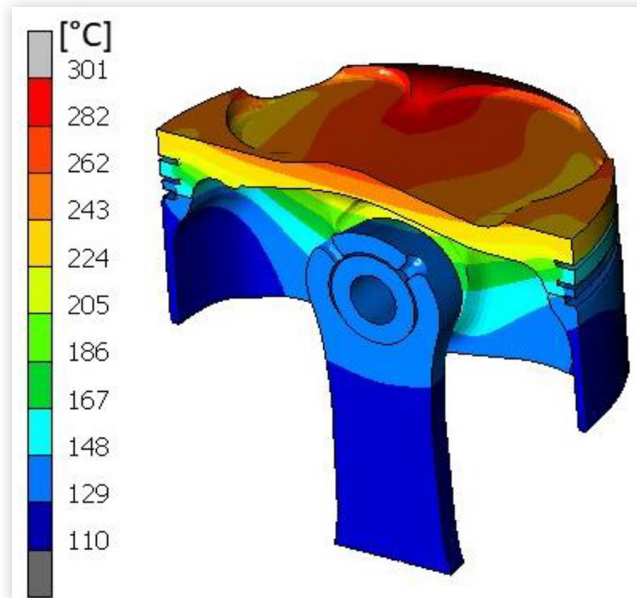
TABLE 2 Material data.

Original Piston	
Material	AlSi9Cu3(Fe)
Thermal conductivity	0.115 W/(mm K)
Density	2.68 kg/dm ³
Young Modulus	73575 MPa
Poisson's ratio	0.3
Thermal expansion coefficient	2.1E ⁻⁵ °C ⁻¹
New piston, gudgeon pin and conrod	
Material	Generic steel
Thermal conductivity	0.039 W/(mm K)
Density	7.8 kg/dm ³
Young Modulus	210000 MPa
Poisson's ratio	0.3
Thermal expansion coefficient	1.1E ⁻⁵ °C ⁻¹

TABLE 3 Thermal boundary conditions.

Crown heat transfer coefficient	0.000667 W/mm °C @1014°C
Piston crown (lateral)	0.000175 W/mm ² °C @90°C
1 st piston ring up heat transfer coefficient	0.002300 W/mm ² °C @90°C
1 st piston ring down heat transfer coefficient	0.005798 W/mm ² °C @90°C
1 st piston ring heat flux	0.0350 W/mm ²
2 nd piston ring up heat transfer coefficient	0.003574 W/mm ² °C @90°C
2 nd piston ring down heat transfer coefficient	0.003977 W/mm ² °C @90°C
Oil ring up heat transfer coefficient	0.002966 W/mm ² °C @90°C
Oil ring down heat transfer coefficient	0.002775 W/mm ² °C @90°C
Skirt heat transfer coefficient	0.008478 W/mm ² °C @90°C
Skirt, intake side, heat flux	0.2076 W/mm ²
Skirt, exhaust side, heat flux	0.1355 W/mm ²
Oil jet heat transfer coefficient	0.005320 W/mm ² °C @120°C
Slashing oil, internal, heat transfer coefficient	0.001856 W/mm ² °C @120°C
Slashing oil, external, heat transfer coefficient	0.000928 W/mm ² °C @120°C
Slashing oil, rod and pin, heat transfer coefficient	0.000773 W/mm ² °C @120°C

FIGURE 4 Temperature contour plot of the crank mechanism, aluminium piston.



Thermal Deformation Analysis of Aluminium Piston

The next step is to retrieve the piston profile of the thermally deformed piston. For this purpose, a different Finite Element thermo-structural model has been set up.

FIGURE 5 Temperature contour plot of the aluminium piston.

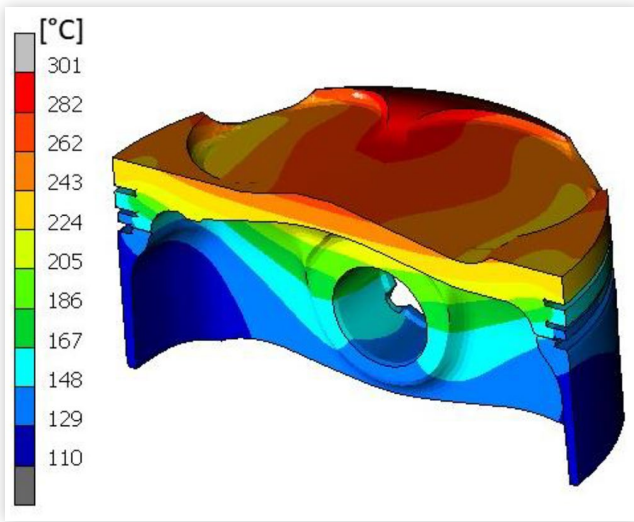


Figure 6 displays the model used and, in particular, the boundary conditions applied are highlighted: symmetry conditions and the constraints useful to properly position the piston in the space have been set up. The temperature field previously computed has been applied starting from a uniform room temperature of 20°C. Figure 7 depicts the result of this simulation in term of x-direction displacement. The piston deformation has been amplified by 10 times and the undeformed piston profile is represented by the thin pink line in the figure. The piston thermal deformation is substantially symmetrical and therefore the behaviour of the piston is similar for the two banks of the L-twin engine. It is easy to see how the truncated conical shape of the crown is deformed under the effect of the thermal field, while to appreciate the deformation of the piston skirt it is necessary to further post-process the output.

Figure 8 shows in detail the difference between the undeformed and the deformed profile of the piston. In particular, the average of the deformation of the profile considering both

FIGURE 6 Structural model for the analysis of the piston profile.

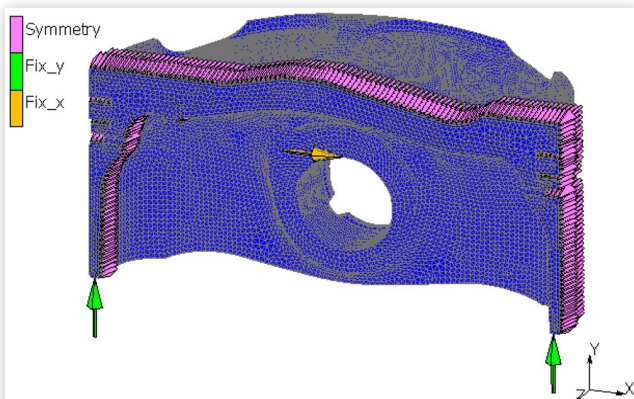


FIGURE 7 x-direction displacement contour plot, aluminium piston.

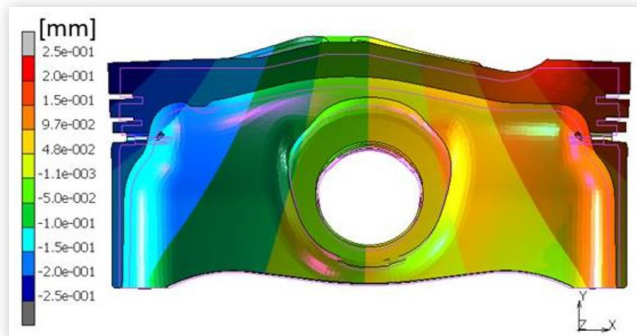
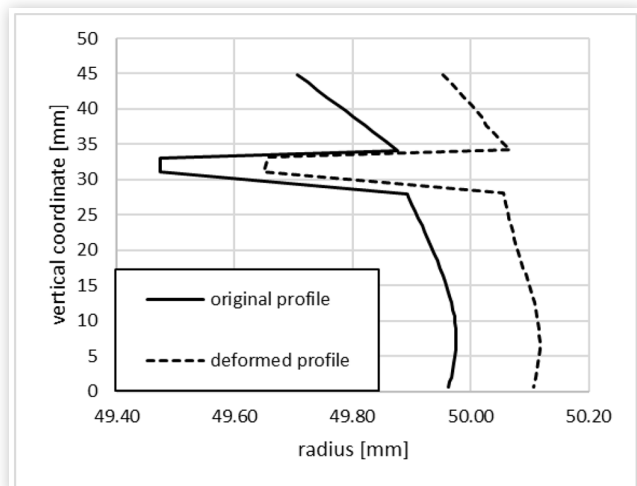


FIGURE 8 Comparison between the cold profile and the hot profile, aluminium piston.

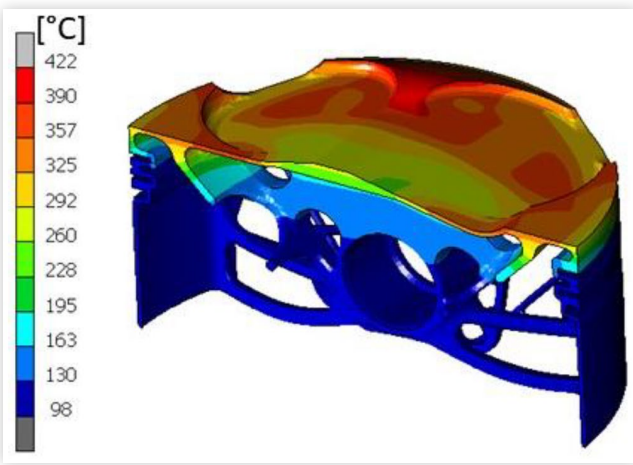


sides of the skirt has been considered. It can be seen how the truncated cone shape of the crown is partially recovered due to thermal effects. Looking at the lower portions of the piston, while the barrel shape of the skirt “opens”, it still offers only one ideal contact point with the liner. These details of the deformed profile have been used to derive a first attempt profile of the steel piston.

Thermal Analysis of Steel Piston

A thermal simulation has been performed to analyse the crank mechanism when the steel piston is considered; the properties of the materials employed are listed in Table 2 and the same boundary conditions retrieved in Table 3 have been applied. Figure 9 shows the result of this simulation. The piston crown reaches a maximum temperature above 400°C in very localized areas and the thermal gradient from the top of the piston to the lower part is stronger than the one registered for the aluminium piston.

FIGURE 9 Temperature contour plot of the steel piston.



Thermal Deformation Analysis of Steel Piston

Successively, a structural model has been set up, quite similar to the one adopted for the aluminium piston. Figure 10 displays the x-direction displacement; the piston deformation has been amplified by 10 times and the undeformed piston profile is represented by a thin pink line. Also in this case, the deformation is almost symmetric.

Figure 11 compares the undeformed cold profile of the new steel piston and the deformed hot one. The initial starting profile of the piston has been considered to be perfectly cylindrical. The next step is to adjust this starting cold profile so that the consequently hot profile is similar to the one of the original aluminium piston.

As a consequence, for each vertical and cylindrical coordinate, the profile of the new steel piston is obtained by:

$$r_{ps} = r_{hs} - r_{ha} \quad (1)$$

where r_{ps} is the radius to be defined for the profile of the steel piston, r_{hs} and r_{ha} are the radii of the hot steel piston and of the hot aluminium one retrieved from the previous thermomechanical simulations.

The nominal diameter of the original aluminium piston is 99.95 mm and it corresponds to the maximum diameter of

FIGURE 10 x-direction displacement contour plot, steel piston.

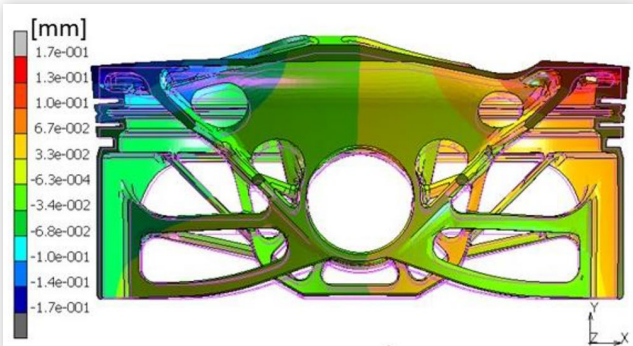
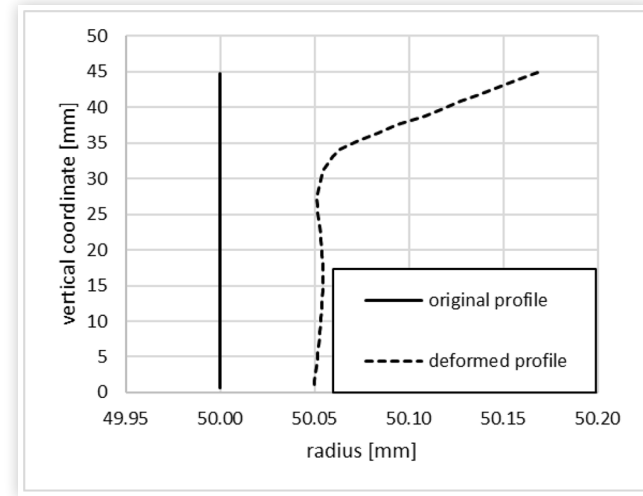


FIGURE 11 Comparison between the cold profile and the hot profile, steel piston.



the cold piston in the lower part of the skirt. The nominal diameter is a vital parameter to be considered in the interaction between the piston and the liner during the engine start phase. In fact, gaps and overclosures heavily affect the distribution of lubricant, the dynamic effect of the secondary motions of the piston and, consequently, the wear of the components involved.

Adopting equation (1), the nominal diameter of the new steel piston should be 100.13 mm. This might mean a reduction of gap in the cold engine or also the onset of a possible overclosure, as a function of the value of the inner diameter of the liner. This crucial aspect will be discussed in detail in the following sections.

A last thermo-structural simulation has been performed to verify the effectiveness of this methodology. Figure 12 shows the thermally deformed profile of both the steel and aluminium piston; a satisfying match has been reached.

FIGURE 12 Comparison between the hot profile of the steel and aluminium pistons.

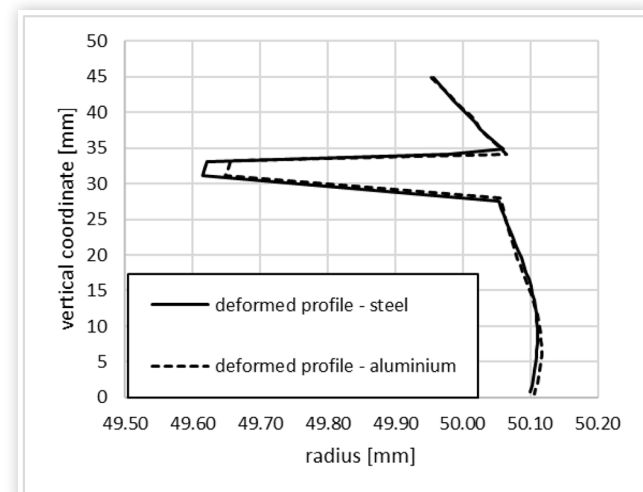
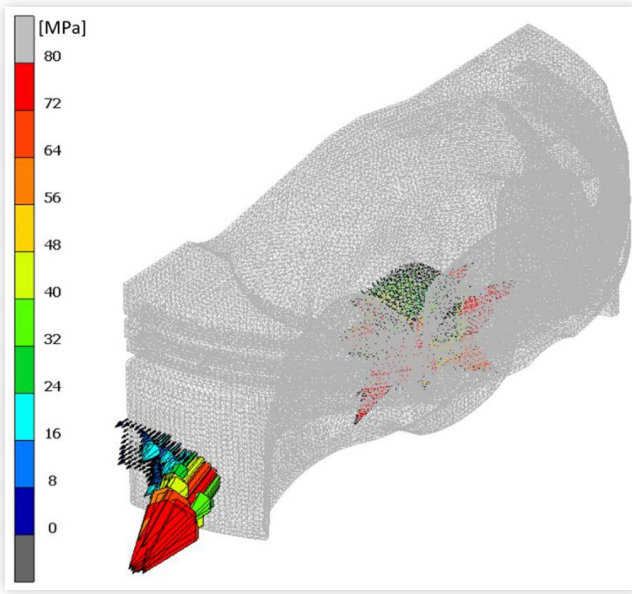
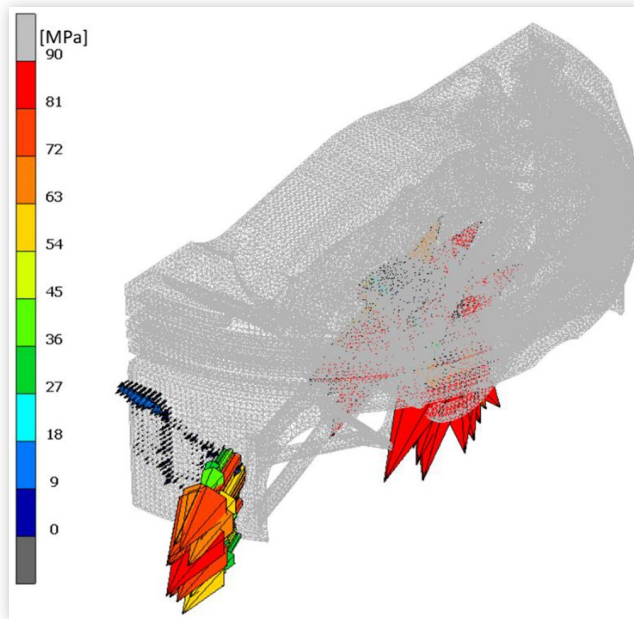


FIGURE 13 Contact pressure vector plot, aluminium piston.**FIGURE 14** Contact pressure vector plot, steel piston.

Thermo-structural Analysis of Aluminium and Steel Piston

At this point, a preliminary thermo-structural simulation has been performed to verify the usefulness of the methodology. A specific Finite Element model has been set up for each piston. The upper part of the crank mechanism has been considered, the instant of maximum piston lateral thrust force has been taken into account and a rigid cylinder liner has been adopted with a diameter of 100.34 mm, considering the nominal diameter of the aluminium liner of 100.014 mm, a thermal expansion coefficient of the liner material of 2.1E⁻⁵ and supposing a homogeneous temperature field of 150°C.

Figure 13 and 14 shows the vector plot of the contact normal pressure for the aluminium and steel piston respectively. Immediately some differences can be noticed. In particular, in the steel piston peaks of pressure are registered at the lateral extremities of the skirt extent thus suggesting further modifications of the piston profile to be needed. Similar considerations will be further discussed in the following sections.

Steel Cylinder Liner Design Process

The definition of the new steel cylinder liner has been much simpler than the process adopted for the steel piston. Figure 15 displays the original aluminium liner where potential contact areas with the engine block are highlighted. In a very preliminary analysis, the structural behaviour of the liner might be mimicked by two simply supported beams loaded by the piston lateral thrust force. Obviously, this is a crude simplification; in fact, the liner could also be seen as a single beam with three supports, but this consideration would lead to a statically

redundant structure thus complicating the next design steps. In addition, a small gap between the contact (light blue) surfaces of Figure 15 and the liner is present so that it is not so easy to understand where the contact is maintained during the application of the load.

It is well known that the majority of failures involving the liner are related to fatigue damage [18,19]. For this reason, the new steel liner has been designed to be structurally equivalent to the aluminium one from the fatigue strength point of view. Therefore, a new steel liner should be designed so that it exhibits the same fatigue safety factor if compared to the aluminium liner when the same loading conditions are considered.

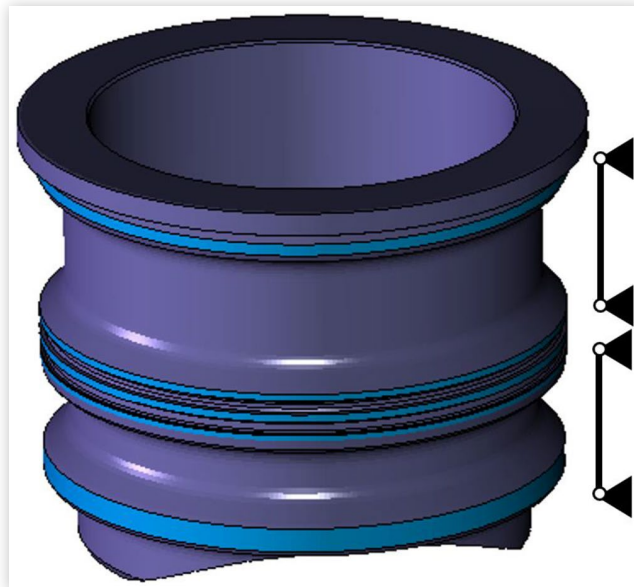
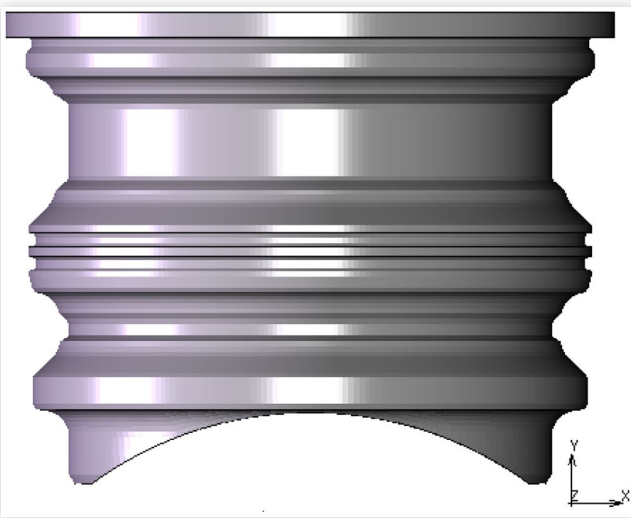
FIGURE 15 The original aluminium cylinder liner.

FIGURE 16 The new steel cylinder liner.



Considering the analogy with a supported beam so far mentioned and the well-known result that in beams bending stress are proportional to the squared value of the local thickness, an initial guess of the radial thickness of the steel liner could be obtained as follow:

$$t_s = t_a \sqrt{\frac{\sigma_{a_lim}}{\sigma_{s_lim}}} \quad (2)$$

where t_a is the thickness of the aluminium liner (4mm), σ_{a_lim} and σ_{s_lim} are the stress limit for a repeated fatigue cycle of aluminium (288 MPa) and steel (512 MPa) respectively and t_s is the resulting thickness (3 mm) of the steel cylinder liner.

Figure 16 shows the new steel cylinder liner. Its shape is quite massive; in fact, the contact areas with the engine block have not been modified thus resulting in a so-called plug and play solution for the engine considered.

Thermal Analysis of the Aluminium Liner

In order to define the nominal internal diameters of both the aluminium and the steel cylinder liners, the thermal field of the liner and its consequent thermal deformation have to be taken into account.

Starting from the original configuration, a Finite Element model of one engine bench has been set up and all the necessary components have been discretized (engine head and block, gasket, bolts and aluminium liner). About 1554 thousand elements have been employed: 177 thousand pentahedral elements (bilinear, 6 nodes, 6 Gaussian integration points), 295 thousand hexahedral elements (bilinear, 8 nodes, 8 Gaussian integration points) and 1082 thousand tetrahedral elements (first order, 4 nodes, one Gaussian integration point). The average element size changes along the model in order to better describe the regions of interest: one millimetre for gasket and elements in contact with it, two millimetres for the liners and four millimetres for the other areas.

A static thermal model has been set up using boundary conditions averaged over the engine cycle. Because of the high

TABLE 4 Material data.

Engine block, head, original liner	
Material	Aluminium
Thermal conductivity	0.115 W/(mm K)
Density	2.68 kg/dm ³
Young Modulus	72000 MPa
Poisson's ratio	0.32
Thermal expansion coefficient	2.1E-5 °C ⁻¹
Bolts, new liner	
Material	Steel
Thermal conductivity	0.039 W/(mm K)
Density	7.8 kg/dm ³
Young Modulus	210000 MPa
Poisson's ratio	0.3
Thermal expansion coefficient	1.1E-5 °C ⁻¹

thermal inertia of metals, the oscillations of walls temperatures due to the cyclic variation of entering heat fluxes have been considered to be negligible [20].

Table 4 collects the material properties of the components used in the model.

Homogeneous boundary conditions have been applied to the oil circuit, to the external surface and to the water jacket of the engine in terms of heat transfer coefficient (HTC) and reference temperature, whose values are specified in Table 5.

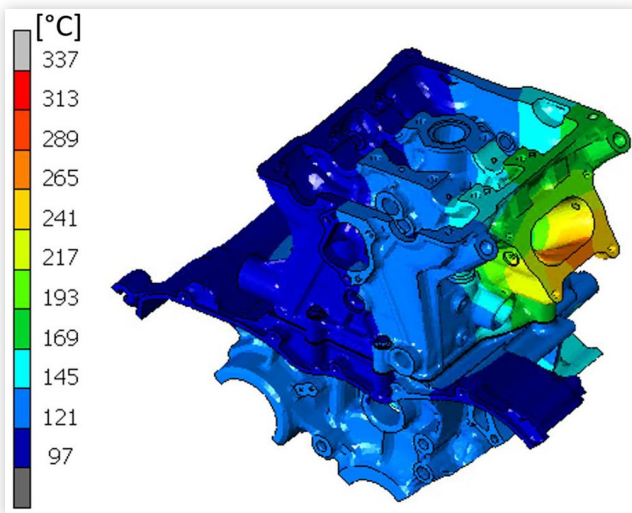
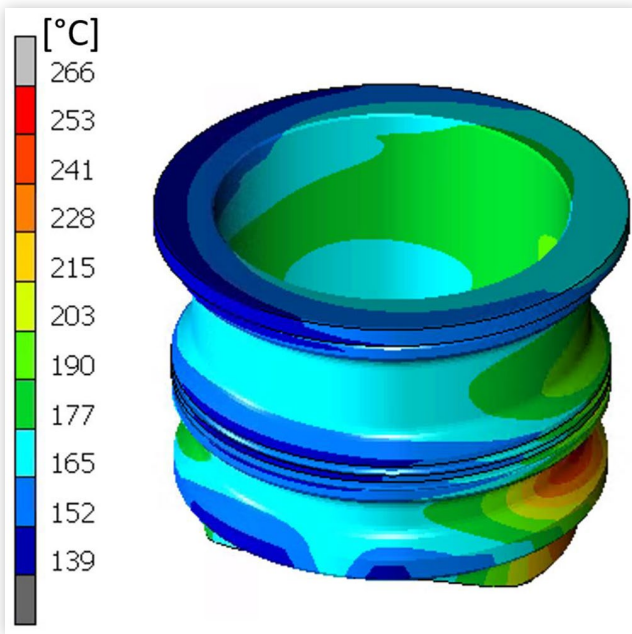
The other boundary conditions have been evaluated using more complex methods following the methodology exposed in [21], at which the interested reader is referred.

The piston alternating motion has been taken into account for the correct estimation of the boundary conditions applied to the liner. Therefore, the effect of the combustion, of the oil and of the heat flux exchanged between the piston and the liner have been inserted using space-dependent tables.

Figure 17 shows the results of the thermal analysis. In particular, Figure 18 represents the temperature contour plot of the liner. The different heat fluxes produced by the piston at the thrust and at the antithrust areas strongly condition the cylinder liner temperature field. Moreover, the lower and

TABLE 5 Thermal boundary conditions.

Oil circuit heat transfer coefficient	0.0003 W/mm ² °C @120°C
External surface heat transfer coefficient	0.000015 W/mm ² °C @40°C
Water jacket heat transfer coefficient	0.002 W/mm ² °C @90°C
Combustion chamber	0.001221 W/mm ² °C @1144°C
Intake duct	0.00014 W/mm ² °C @32°C
Exhaust duct	0.00026 W/mm ² °C @727°C
Combustion heat transfer coefficient	Tables for HTC and temperature
Coolant oil	Table for HTC @120°C, maximum value of 0.0003 W/mm ² K
Conduction heat flux	Table
Intake side heat flux	Table
Exhaust side heat flux	Table

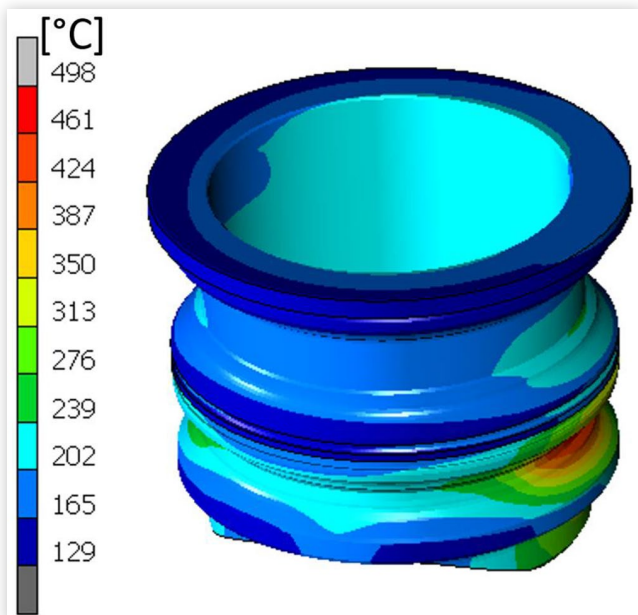
FIGURE 17 Temperature contour plot of one engine bench.**FIGURE 18** Temperature contour plot of the aluminium liner.

hottest part of the liner is not in contact with the cooling water. Therefore, this temperature distribution along the liner is strongly non-axisymmetric and inhomogeneous.

Thermal Analysis of the Steel Liner

A Finite Element model similar to the one just described has been set up replacing the aluminium liner with the steel one.

Figure 19 shows the temperature contour plot of the steel liner. A definitely higher peak of temperature is located in the lower part of the liner when compared to the aluminium liner temperature field of Figure 18. This result is caused by the

FIGURE 19 Temperature contour plot of the steel liner.

different thermal conductivity of the materials. In particular, thermal conductivity of steel ($0.039 \text{ W}/(\text{mm K})$) is almost one third of the thermal conductivity of aluminium ($0.157 \text{ W}/(\text{mm K})$). Moreover, the high-temperature peak is located in the lower area, where the effect of the cooling water is absent, so the thermal path starting from the lower part of the liner encounter a huge resistance when it tries to move axially toward the upper part of the liner in contact with the water, also considering that the steel liner has a thinner radial thickness than the aluminium one. These results suggest that the sole structural equivalence alone cannot properly guide the design of a new steel liner and the temperature contour plot indicates that a deeper redesign of the engine block and of the water jacket should be performed, which is out of the scope of the present contribution.

Thermal Deformation Analysis of Steel Liner

Finally, the nominal diameter of the internal bore of the steel liner has to be defined. In particular, the thermally deformed internal bore of the steel liner should be similar to the one of the original aluminium one since the steel piston profile has been designed to reach the same hot profile as the original aluminium piston. In this way, it should be possible to combine these four components thus obtaining four different coupling configurations. In addition, no critical issue should be encountered during the operating conditions since the gap of the original configuration (aluminium piston and aluminium liner) should have been kept also in the other three new configurations.

The nominal bore diameter of the steel liner, d_s , has been calculated as follow:

$$d_s = d_a \frac{1 + \alpha_a \Delta T_a}{1 + \alpha_s \Delta T_s} \quad (3)$$

where d_a is the diameter of the aluminium liner (100.014 mm), α_a and α_s are the thermal expansion coefficient of aluminium ($2.1 \times 10^{-5} \text{C}^{-1}$) and steel ($1.1 \times 10^{-5} \text{C}^{-1}$) respectively, ΔT_a and ΔT_s are the computed average delta temperature of the inner surface of the aluminium (156°C) and steel (206°C) liner respectively. The nominal bore diameter of the steel liner, d_s , results out to be 100.116 mm.

Thermo-structural Analysis of the Engine

Once the geometries of the steel piston and steel liner have been defined, contact interactions between these components have been analysed adopting Finite Element numerical simulations.

In particular, simulations that involve a whole engine bench are very heavy from a computational point of view so that suitable simplified methodologies have been developed to speed up these models.

In the present paper, the methodologies described in [21,22] have been adopted, at which the interest reader is referred, and they are briefly summarised in the following for the sake of clarity.

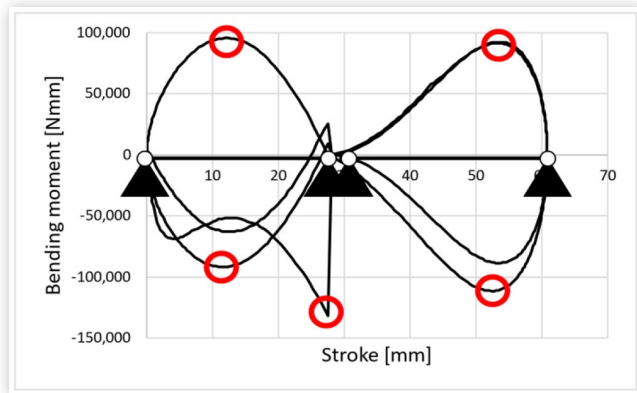
Preliminarily, a static thermomechanical non-linear simulation of the assembly of one bench of the engine has been performed. In particular two instances of the engine cycle have been mimicked: a state of null chamber pressure and the condition of maximum chamber pressure (91 bar).

These simulations aimed at computing the contact normal pressures generated by the gasket on the liner flange and on the deck during the operating condition when these reach their maximum values (null chamber pressure) and when these reach their minimum values (maximum chamber pressure). In fact, the chamber pressure tends to separate the engine head from the engine block thus resulting in a reduction of the contact pressure acting on the engine deck.

Therefore, these two simulations represent the border conditions of all the possible intermediate configurations based on the chamber pressure. In particular, a high number of simulations would be required to study the liner in the two material configurations, so that to adopt a methodology to speed up this phase is mandatory.

The first validation of the design of the piston-liner coupling has consisted of fatigue analyses of the liner for each one of the possible four configurations considered. First of all, it has been necessary to identify the border of the fatigue cycle. In a preliminary phase, the piston thrust profile has been taken into account, but it has been evident that the value of thrust force alone cannot identify the fatigue cycle since the stress status of the liner also dependent on the instantaneous position of the piston. Thus, again referring to the simplified supported beam approximation of the liner, see Figure 15, the corresponding bending moment profile has been estimated, see Figure 20. Five different local maxima or minima have been identified, in red in Figure 20, and employed to identify the corresponding static mechanical analysis to be performed.

FIGURE 20 Bending moment profile, the five load cases are highlighted in red.



For each of these five loadcases, a simplified model has been performed. Only the engine block, liner and bolts have been considered. The contact pressure between gasket and engine block has been applied directly to the engine deck and to the liner flange while the corresponding tightening force has been applied directly to a cross-section of the bolts. The value of these boundary conditions has been retrieved from the previous two complete simulations adopting a simple linear interpolation:

$$a_\theta = (a_{max} - a_{min}) \frac{p_\theta - p_{min}}{p_{max} - p_{min}} + a_{min} \quad (4)$$

where p_θ is the chamber pressure at the specific loadcase considered, p_{max} and p_{min} are the maximum and minimum chamber pressure registered along the whole engine cycle, a_θ represents the generic physical quantity to be computed (the value of the pressure acting on the liner flange or on the deck or the tightening force acting on the bolts) and a_{max} and a_{min} are the values of the same physical quantity registered at the condition of maximum and minimum chamber pressure respectively.

In addition, for each loadcase, the crank mechanism has been inserted, correctly positioned, the rod has been properly tilted and the necessary boundary conditions have been applied (thermal field, acceleration and gas pressure).

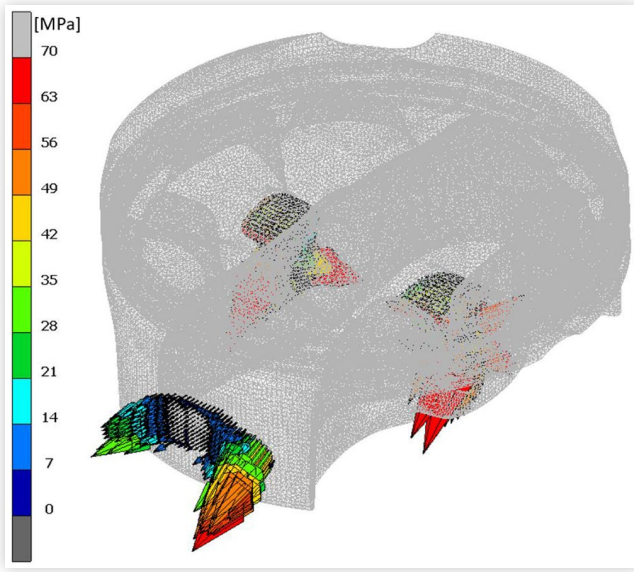
To sum up, twenty simplified simulations have been performed, five for each one of the four possible configurations based on the materials adopted for the piston and for the liner.

Results of the Thermo-structural Analyses and Discussion

Aluminium Piston and Aluminium Liner

This is the actual configuration of the engine studied, therefore no critical issue should be detected. The cold maximum diameter of the aluminium piston is 99.95 mm, while the cold

FIGURE 21 Contact pressure vector plot, aluminium piston and aluminium liner.

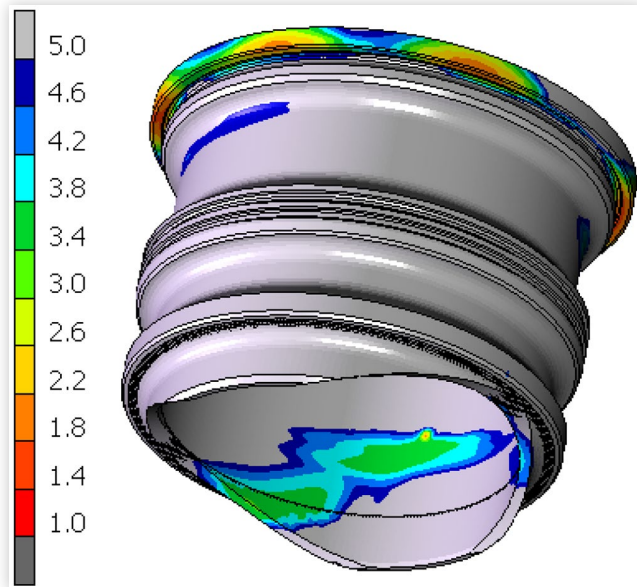


bore of the aluminium liner is 100.014 mm so that a radial gap is present in the cold start phase of the engine. In addition, the numerical forecasts show that no overclosure is registered in any of the five load cases thus suggesting that the necessary film of lubricant oil should be always present during the operating conditions.

Figure 21 shows the maximum value contact pressure among the five load cases simulated. The peaks are correctly located in the area of the skirt directly supported by the bosses and the contact area, Figure 22, is positioned in the lower-central part of the skirt.

Figure 23 depicts the safety factor contour plot of the liner, where the multiaxial Dang Van criterion has been adopted [23]. No critical parts are visible, in fact, the lower values exceed the value of 1.8 everywhere.

FIGURE 23 Dang Van fatigue safety factor contour plot, aluminium piston and aluminium liner.



Aluminium Piston and Steel Liner

In this second configuration, the aluminium liner has been replaced by the steel one. The cold maximum diameter of the aluminium piston is still 99.95 mm, while the cold bore of the steel liner has been set equal 100.116 mm, following results presented at previous sections. Therefore, a higher gap during the cold start phase is present if compared to the original configuration. This could lead to a not optimal distribution of the lubricant between the liner and the piston. In fact, the piston profile is designed to ensure a correct hydrodynamic pressure also considering the gap with the liner. In addition, the contact interaction between the skirt and liner during the operating condition must be analysed.

FIGURE 22 Contact status contour plot, aluminium piston and aluminium liner.

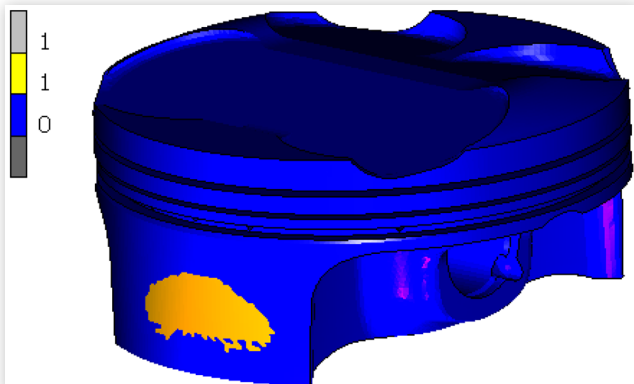


FIGURE 24 Contact pressure vector plot, aluminium piston and steel liner.

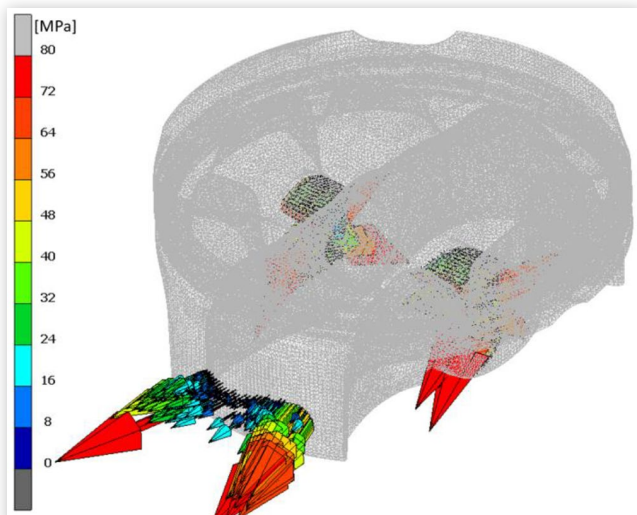


FIGURE 25 Contact status contour plot, aluminium piston and steel liner.

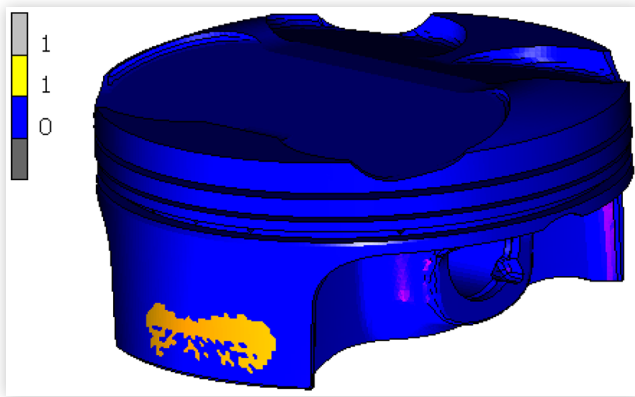
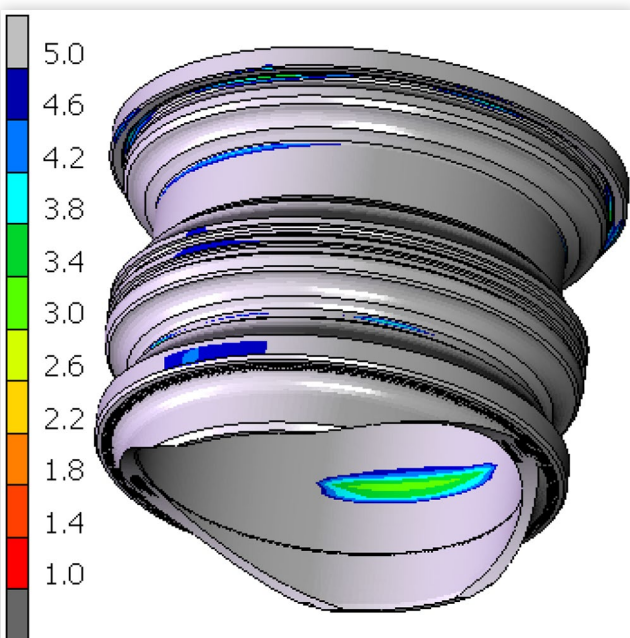


Figure 24 shows the contact pressure vector plot. Even if the maximum values of the pressure are correctly located in the lower part of the piston, they are almost doubled if compared to the ones shown in Figure 21. This is obviously connected to a much more irregular contact area, see Figure 25. This evidence is probably linked to a too rigid liner and this high value of contact pressure could lead to a disruption of the lubricant film, thus producing damages to the piston and to the liner.

Figure 26 depicts the safety factor contour plot of the liner. Very high values are the consequence of the massive geometry of this component. As a consequence, it could be possible to reduce the thickness of the liner; hopefully, it might improve the shape of the contact area and decrease the value of the peaks of contact pressure.

FIGURE 26 Dang Van fatigue safety factor contour plot, aluminium piston and steel liner.



Steel Piston and Aluminium Liner

In this third configuration, the steel piston and the aluminium liner have been considered. The cold maximum diameter of the steel piston is 100.13 mm, see previous sections, while the cold bore of the aluminium liner is 100.014 mm. Therefore, a considerable overlap is present during the cold start phase so that it would be mandatory to warm up the engine before the cold start phase (similar procedures are employed for race engines). Figure 27 shows the contact pressure vector plot. Even if the maximum values of the pressure are correctly located in the lower part of the piston, contact is detected also in the upper part of the skirt, see Figure 28. These results point out the necessity to slightly correct the profile of the steel piston. It could be also necessary to increase the ovality of the skirt; in fact, the central part of the skirt shrinks from supporting the load and a more pronounced elliptical shape might promote a better distributed pressure vector plot. In particular, the geometry of the pin bosses of the steel piston

FIGURE 27 Contact pressure vector plot, steel piston and aluminium liner.

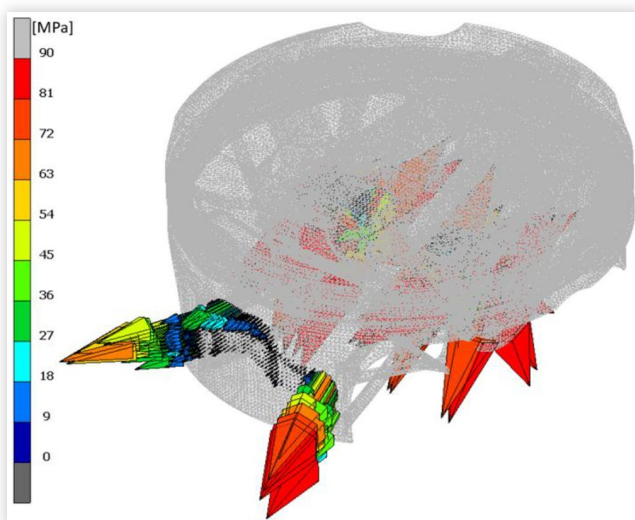


FIGURE 28 Contact status contour plot, steel piston and aluminium liner.

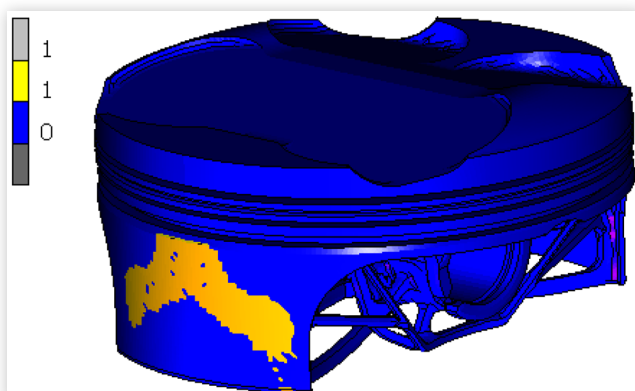
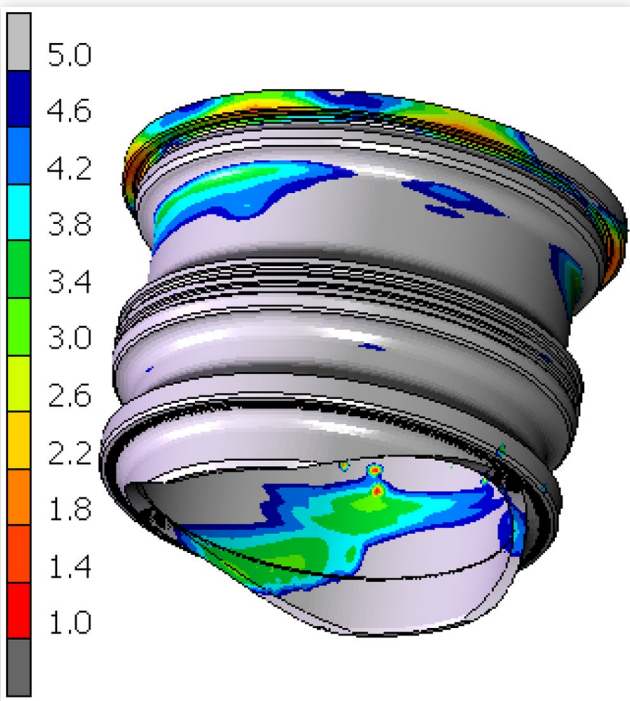


FIGURE 29 Dang Van fatigue safety factor contour plot, steel piston and aluminium liner.



is very different from the aluminium one so that trying to calculate the ovality is clearly unprecise under the assumption that the pin bosses of these two different pistons exhibit the same stiffness. Therefore, an iterative correction of the elliptical shape is mandatory to reach a suitable contact interaction.

Figure 29 displays the safety factor contour plot of the liner. Very localized potentially critical areas are present in the lower part of the liner, even if the safety factor is never lower than 1. These low values are probably generated by the peaks of the contact pressure so that a correction of the piston profile might have a beneficial effect on both the involved components.

Steel Piston and Steel Liner

In this last configuration, the steel piston and the steel liner are involved. The cold maximum diameter of the steel piston is 100.13 mm, while the cold bore of the steel liner is 100.116 mm so that a small overlap can be noticed during the cold start phase. This result could be counterintuitive; in fact, it could be easy to suppose that a gap at room temperature should guarantee a gap also at high temperatures when the same material for the piston and for the liner is involved. However, the thermal simulations have shown that the skirt of the steel liner reaches an operating temperature that is lower than the operating temperature of the liner. Therefore, also in this configuration, it is necessary to warm up the engine block and liners before the starting phase. To avoid this annoying procedure, it is necessary to properly design the cylinder liner and the water jacket. The liner should exhibit a lower thickness and the water jacket should wet and cool down also the lower part of the liner. If the operating condition of

FIGURE 30 Contact pressure vector plot, steel piston and steel liner.

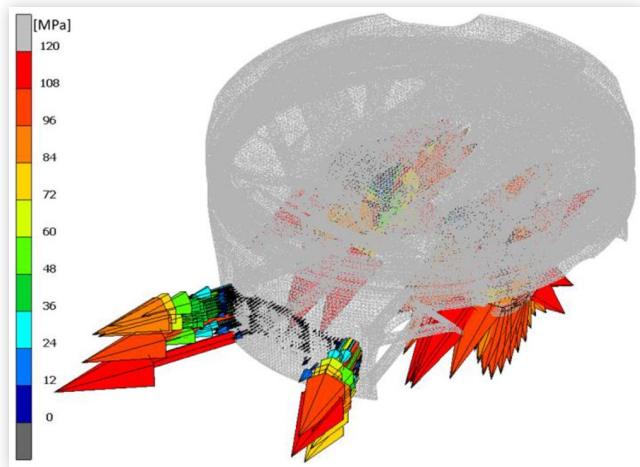
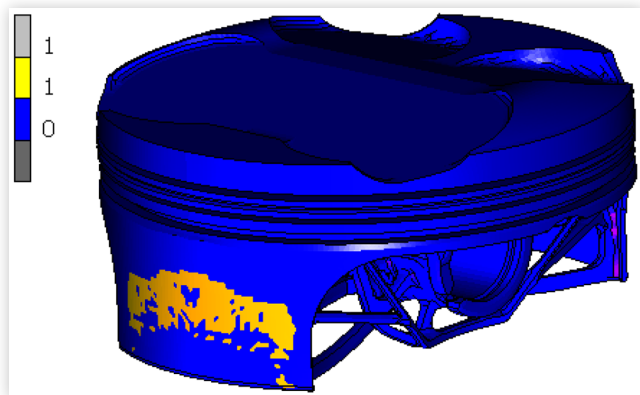


FIGURE 31 Contact status contour plot, steel piston and steel liner.



the liner is reduced, it would be possible to adopt a larger cold bore of the liner.

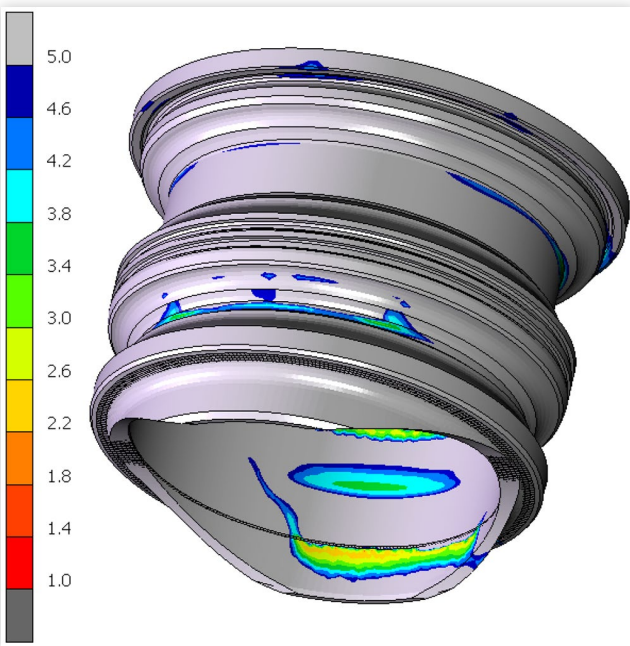
Figure 30 and 31 describe almost the same issues encountered in the previous configuration, even if the contact in the upper region of the skirt is now absent.

Figure 32 displays the safety factor contour plot of the steel liner. The values are always higher than 2.2, thus confirming the possibility to thin the radial thickness of the liner.

Conclusions and Future Works

In the present contribution, a methodology to design a steel piston and a steel liner has been described for a specific engine configuration. In particular, the main focus was the contact interaction between the piston and the liner when different materials, aluminium and steel, were employed. The original engine adopted both these components made of aluminium. The first step was to define the profile of a possible steel piston

FIGURE 32 Dang Van fatigue safety factor contour plot, steel piston and steel liner.



to obtain the same thermally deformed shape of the skirt when compared to the aluminium piston. Afterwards, the geometry of the steel liner was defined; in particular, the internal bore was calculated to exhibit the same diameter if compared to the aluminium one during the operating condition.

These components were analysed using numerical tools; in particular, four different configurations were investigated: piston and liner made of aluminium, aluminium piston and steel liner, steel piston and aluminium liner and, finally, both piston and liner made of steel. The main aspects analysed in the results have been the presence of gap or overlap, the distribution of the contact pressure, the extent and position of the contact area and the fatigue life safety factor of the liner. Obviously, the original configuration of the aluminium piston and liner did not exhibit any critical issue. The second configuration, aluminium piston and steel liner, showed a wide gap when the cold engine condition was taken into account. Therefore, the lubricant oil distribution could not be optimal during the first engine cycles. The fatigue analysis of the stell liner did not show any issue, thus suggesting the possibility to further thin this component. The third configuration, steel piston and aluminium liner, showed a strong overlap between these two components during the cold start. Preheating the liner and the block before starting the engine appeared to be mandatory, thus limiting this application to the racing cars field. This third configuration displayed also the necessity to correct the oval shape of the piston, which could not be simply retrieved from the original aluminium piston. Iterative cycles of geometry modifications and Finite Element verifications should be performed. Also the last fourth configuration, steel piston and steel liner, displayed that the steel piston ovality should be increased. In addition, a small overlap was present at room temperature, thus suggesting to correct the external shape of the steel liner and the water jacket to be modified in

order to properly cool down the lower part of the liner thus allowing a larger cold bore to be designed.

Future works should include an experimental validation of the results obtained. First, the static and fatigue strength of the designed steel piston must be checked. It could be possible to insert the new piston directly into the engine with the original aluminium cylinder liner, but there would be an unnecessary risk of seriously damaging the entire engine. Instead, an ad hoc test rig could be built, in which the crank mechanism moves inside a simplified cylinder liner and the pressure exerted by combustion is simulated by a compressible body placed on the top of the piston. Secondly, it would be necessary to test in detail the contact interaction between piston and cylinder liner in the four configurations according to the different materials used. Finally, it is necessary to test the four possible configurations in the actual engine and investigate in detail the cylinders and pistons looking for breakages, damages or polishings of the components that could be the consequence of too high contact pressures and therefore a probable symptom of not sufficiently suitable piston profiles.

Further analysis could be performed to consider also the different dynamic effects based on the different configuration adopted. In fact, the gap strongly affects the secondary motions of the piston. In particular, the simplified methodology exposed in [24] would speed up also this possible last phase.

References

1. MAHLE, "Piston Materials, Pistons and Engine Testing," Springer Fachmedien Wiesbaden, Wiesbaden, ISBN 9783834815903: 59-81, 2016, doi:[10.1007/978-3-658-09941-1_4](https://doi.org/10.1007/978-3-658-09941-1_4).
2. Ahmed, A., Wahab, M.S., Raus, A.A., Kamarudin, K. et al., "Mechanical Properties, Material and Design of the Automobile Piston: An Ample Review," *Indian J. Sci. Technol.* 9, no. 36 (2016), doi:[10.17485/ijst/2016/v9i36/102155](https://doi.org/10.17485/ijst/2016/v9i36/102155).
3. Rajakumar, S. and Karthiyaraj, M., "A Comparative Study of Structural and Thermal Analyses on Piston Materials," *Int. J. Sci. Dev. Res.* 5, no. 12 (2020): 208-212.
4. Singh, U., Lingwal, J., Rathore, A., Sharma, S. et al., "Comparative Analysis of Different Materials for Piston and Justification by Simulation," *Mater. Today Proc.* 25 (2020): 925-930, doi:[10.1016/j.matpr.2020.03.078](https://doi.org/10.1016/j.matpr.2020.03.078).
5. Schreer, K., Roth, I., Schneider, S., and Ehnis, H., "Analysis of Aluminum and Steel Pistons—Comparison of Friction, Piston Temperature, and Combustion," *J. Eng. Gas Turbines Power* 136, no. 10 (2014): 101506, doi:[10.1115/1.4027275](https://doi.org/10.1115/1.4027275).
6. Pierce, D., Haynes, A., Hughes, J., Graves, R. et al., "High Temperature Materials for Heavy Duty Diesel Engines: Historical and Future Trends," *Prog. Mater. Sci.* 103, no. January 2018 (2019): 109-179, doi:[10.1016/j.pmatsci.2018.10.004](https://doi.org/10.1016/j.pmatsci.2018.10.004).
7. Gray, J. and Depcik, C., "Review of Additive Manufacturing for Internal Combustion Engine Components," *SAE Int. J. pmatsci.*

- Engines* 13, no. 5 (2020): 03-13-05-0039. <https://doi.org/10.4271/03-13-05-0039>.
8. MAHLE, "Cylinder Components," Vieweg+Teubner, Wiesbaden, ISBN 978-3-8348-0785-4, 2010, doi:[10.1007/978-3-8348-9697-1](https://doi.org/10.1007/978-3-8348-9697-1).
 9. Schneider, E.W., Blossfeld, D.H., Lechman, D.C., Hill, R.F. et al., "Effect of Cylinder Bore Out-of-Roundness on Piston Ring Rotation and Engine Oil Consumption," SAE Technical Paper Series (1993), <https://doi.org/10.4271/930796>.
 10. Reddy Kummitha, O. and Reddy, B.V.R., "Thermal Analysis of Cylinder Block with Fins for Different Materials Using ANSYS," *Mater. Today Proc.* 4, no. 8 (2017): 8142-8148, doi:[10.1016/j.matpr.2017.07.155](https://doi.org/10.1016/j.matpr.2017.07.155).
 11. Reddy Anugu, A., Vishnu Tej Reddy, N., and Venkateswarlu, D., "Theoretical Modelling and Finite Element Analysis of Automobile Piston," *Mater. Today Proc.* 45, no. xxxx (2021): 1799-1803, doi:[10.1016/j.matpr.2020.08.741](https://doi.org/10.1016/j.matpr.2020.08.741).
 12. Mansouri, S.H. and Wong, V.W., "Effects of Piston Design Parameters on Piston Secondary Motion and Skirt - Liner Friction," *Proc. Inst. Mech. Eng. Part J J. Eng. Tribol.* 219, no. 6 (2005): 435-449, doi:[10.1243/135065005X34026](https://doi.org/10.1243/135065005X34026).
 13. Totaro, P.P., Westerfield, Z., and Tian, T., "Introducing a New Piston Skirt Profile to Reduce Engine Friction," SAE Technical Papers (2016), <https://doi.org/10.4271/2016-01-1046>.
 14. Zhu, D., Pritchard, E.G.D., and Silverberg, L.M., "A New System Development Framework Driven by a Model-Based Testing Approach Bridged by Information Flow," *IEEE Syst. J.* 12, no. 3 (2018): 2917-2924, doi:[10.1109/JSYST.2016.2631142](https://doi.org/10.1109/JSYST.2016.2631142).
 15. Barbieri, S.G., Giacopini, M., Mangeruga, V., and Mantovani, S., "A Design Strategy Based on Topology Optimization Techniques for an Additive Manufactured High Performance Engine Piston," *Procedia Manuf.* 11 (2017): 641-649, doi:[10.1016/j.promfg.2017.07.162](https://doi.org/10.1016/j.promfg.2017.07.162).
 16. Barbieri, S.G., Giacopini, M., Mangeruga, V., and Mantovani, S., "Design of an Additive Manufactured Steel Piston for a High Performance Engine: Developing of a Numerical Methodology based on Topology Optimization Techniques," *SAE Int. J. Engines* 11, no. 6 (2018): 2018-01-1385. <https://doi.org/10.4271/2018-01-1385>.
 17. Cantore, G., Giacopini, M., Rosi, R., Strozzi, A. et al., "Validation of a Combined CFD / FEM Methodology for the Evaluation of Thermal Load Acting on Aluminum Alloy Pistons through Hardness Measurements in Internal Combustion Engines," 29 (2011).
 18. Malakizadi, A., Chamani, H., Shahangian, S.N., Jazayeri, S.A. et al., "Thermo-mechanical Fatigue Life Prediction of a Heavy Duty Diesel Engine Liner," no. November 2014 (2009): 529-535, doi:[10.1115/icef2007-1775](https://doi.org/10.1115/icef2007-1775).
 19. Branco, C.M., Infante, V., Sousa, E., Brito, A. et al., "A Failure Analysis Study of Wet Liners in Maritime Diesel Engines," *Eng. Fail. Anal.* 9, no. 4 (2002): 403-421, doi:[10.1016/S1350-6307\(01\)00027-9](https://doi.org/10.1016/S1350-6307(01)00027-9).
 20. Fontanesi, S. and Giacopini, M., "Multiphase CFD-CHT Optimization of the Cooling Jacket and FEM Analysis of the Engine Head of a V6 Diesel Engine," *Appl. Therm. Eng.* 52, no. 2 (2013): 293-303, doi:[10.1016/j.applthermaleng.2012.12.005](https://doi.org/10.1016/j.applthermaleng.2012.12.005).
 21. Barbieri, S.G., Giacopini, M., Mangeruga, V., Bianco, L. et al., "A Simplified Methodology for the Analysis of the Cylinder Liner Bore Distortion: Finite Element Analyses and Experimental Validations," SAE Technical Paper Series (2019), <https://doi.org/10.4271/2019-24-0164>.
 22. Barbieri, S.G., Mangeruga, V., Giacopini, M., Laurino, C. et al., "A Finite Element Numerical Methodology for the Fatigue Analysis of Cylinder Liners of a High Performance Internal Combustion Engine," *Key Eng. Mater.* 827 (2019): 288-293, doi:[10.4028/www.scientific.net/kem.827.288](https://doi.org/10.4028/www.scientific.net/kem.827.288).
 23. Dang Van, K., Cailletaud, G., Flavenot, J.F., Le Douaron, A., and Lieurade, H.P., "Criterion for High Cycle Fatigue Failure under Multiaxial Loading," *Biaxial and Multiaxial Fatigue*, 459-478, 1989.
 24. Barbieri, S.G., Bianco, L., Mangeruga, V., and Giacopini, M., "A Simplified Finite Element Methodology for the Structural Assessment of an Engine Piston under Dynamic Loadings," 020014 (2020), doi:[10.1063/5.0033956](https://doi.org/10.1063/5.0033956).

Contact Information

Saverio Giulio Barbieri

Engineering Department "Enzo Ferrari", University of Modena and Reggio Emilia, via Vivarelli 10, 41125 Modena, Italy

saveriogiulio.barbieri@unimore.it

Definitions/Abbreviations

ps - profile of the steel piston

hs - hot profile of the steel piston

ha - hot profile of the aluminium piston

s - steel

a - aluminium

HTC - heat transfer coefficient